

Impact of newly synthesized water soluble photoluminescent ZnS-L-Cysteine: Core-shell nanoparticles in defining the *in-situ* opto-electronic orbital model

Vaishali Shukla¹, Bhargav Raval¹, Man Singh^{1,2*}

¹School of Nanoscience, Central University of Gujarat, Gandhinagar 382030, India

²School of Chemical Sciences, Central University of Gujarat, Gandhinagar 382030, India

*Corresponding author. Tel: (079)-23260210; E-mail: vshukla2112@gmail.com, mansingh50@hotmail.com

Received: 10 September 2016, Revised: 26 October 2016 and Accepted: 22 November 2016

DOI: 10.5185/amlett.2017.7078

www.vbripress.com/aml

Abstract

An intermolecular charge and electron transfer processes in photo luminescent ZnS- L-Cysteine: core-shell Nanoparticles (NPs) extend highly sensitive and variable valence at the core (ZnS)-shell (L-Cysteine) interface primarily due to an extensive mixing of materials frontier orbital (i.e. covalency). Water soluble, ZnS- L-Cysteine: core-shell photo luminescent NPs achieved by straightforward micellar route that is thrust area of research in nanoscience for the control particle size and remarkable properties through chemical co-precipitation method. In the paper we studied, the synthesis of CTAB capped ZnS NPs as well ZnS- L Cysteine: core-shell NPs and examined by their composition, particle size and optical and luminescent properties. The NPs stabilized with CTAB and demonstrated the regular ZnS blue emission on recombination over ZnS band-crevice from shallow electron traps at 490 nm. The onset of the absorption was 80 nm blue shifts moved from 345 nm (bulk) to 265 nm, showing a quantum size impact. Quantum mechanical effect of light applied especially in semiconducting NPs through optoelectronic orbital model, which detect and control the light through electronic devices. Copyright © 2016 VBRI Press.

Keywords: Opto-electronic orbital model, quantum mechanical effect, micellar route, ZnS-L-Cysteine, core-shell NPs.

Introduction

Zinc sulphide (ZnS), a typical II-VI semiconducting compound is a promising optoelectronics devices material because of its wide direct band gap (3.5 - 4.00 eV). Thus, the new changes could happen as one advances from functional to super functional ions of nanomaterials (NMs) comprising of a countable number of molecules to proposed application. For example, nanocrystalline semiconductor accumulated for maximum surface area with least potential energy that becomes a natural barrier overall surface of targeted material. Therefore, NMs incorporate the methodology, designing, optical strength to transfer the potential energy into the kinetic energy due to non-accumulated particles of the surface in context of relative properties. In general, NPs with least potential energy could facilitate the bulk materials in the on-going process to attain functionalized state. However, despite such a unique and novelty capping on ZnS NPs with cationic surfactant like Cetyl trimethyl ammonium bromide (CTAB) *via* micellar route and functionalization of NM with metallic to biomolecules, no effective research is reported yet. Thus, our initiation in developing NMs using CTAB capped ZnS NPs with L-Cysteine shell in aqueous medium following green chemical process could pioneer concept for advance research [1].

Core-shell structured NPs are a type of biphasic materials that have an inner core structure and an outer shell made of different components. These NPs have been interest as they can exhibit unique properties arising from the combination of core and shell material, geometry, and design due to sulphur atom (S^{2-}) support linkage with quaternary nitrogen atom (N^+), and which gives void space on the particle surface of core-shell NPs used as carrier [2]. Reportedly, the photoluminescence (PL) mechanism of ZnS nanocrystals covered with other shell materials is extremely intricate. To start with, PL based process the NPs have higher surface to volume ratio where more surface area contain open bearers for PL. This shows that surface states are vital with unique physicochemical properties, particularly the optical, luminescence and optoelectronics properties. Generally, semiconductor NPs has excitonic and trapped luminescence. The sharp excitonic emission situated close to the absorption edge of the particles, while the trapped emission is wide and feeds moved. Just the trapped luminescence emerging from the surface states which seen in the Core-Shell ZnS NPs [3]. Additionally, the fluorescent II-VI semiconductor core-shell NPs have pulled in extraordinary interests as compared to reported material decade because of their potential applications

going from photonics [4] to biophotonics devices [5]. Biodynamic shell coated ZnS semiconductor nanocrystals have been encouraging to begin with new bio mark with photo stability, expansive stokes move and well water dissolvability. In addition, the chemical nature of bioactive shell material in aqueous solution, the luminescence of the nanocrystal is delicate to temperature and pH value [6]. The majority of NPs and core-shell NPs is synthesized using phase synthesis techniques usually involve chemical vapor deposition (CVD) and Sol-Gel route. [2, 3]. However, these techniques also involve multiple steps, usually depositing the shell material onto an already formed core structure, and use substrates [7-9]. These established techniques, investigated mechanism and various parameters affect on the formation particles [10]. Thereby, efficient technique was developed to coating L-Cysteine as natural shell particles to functionalize CTAB capped ZnS NPs. L-Cysteine coated ZnS NPs (ZnS-L-Cysteine NPs) incorporated in CTAB micellar solution are best suitable as far as yield and size appropriation; on the other hand carboxylic hydrophilic group (-COOH) is available on the particle surface making them soluble in aqueous solution. To minimize the coagulation of the core NPs, CTAB utilized to change the nanocrystal surface and the ideal adjustment condition was resolved. The ZnS-L-Cysteine: core-shell NPs are sufficiently vigorous to oppose acid carving and keep up photoluminescence properties with charge alignment depicted to zeta-potential [11-13].

In this paper, we gave an account of a fruitful synthesis of CTAB capped ZnS NPs and ZnS- L-Cysteine: Core-Shell NPs via new micellar route using chemical precipitation method. In this method, the core-shell NPs synthesized directly in one-step without substrates. The precursors chemical compounds used are in the form of aqueous micelles capped molecules, which further degraded into the final core or shell NMs. Thus, this method may also be a more economical method of synthesizing certain types of core-shell NPs. Previously; nanopowders synthesized with this method have at kg/h rate [14-16]. X-ray diffraction (XRD), Fluorescence Spectroscopy, IR-Spectroscopy (FTIR), UV-Spectroscopy, Thermal gravimetric analysis (TGA) and scanning electron microscopy (SEM) tools used to characterize prepared NPs.

Experimental

Synthesis of CTAB capped ZnS NPs and ZnS- L-Cysteine: Core-Shell NPs carried out at RT using a simple chemical precipitation route with micelles capping as described by Shukla *et al.* [1].

Materials

To synthesize CTAB (cationic surfactant) capped ZnS NPs and ZnS-L-Cysteine: Core-Shell NPs, the following materials used. Zinc Sulphate heptahydrate ($\text{ZnSO}_4 \cdot 7\text{H}_2\text{O}$), Sodium Sulphide ($\text{Na}_2\text{S} \cdot x\text{H}_2\text{O}$), Cetyl trimethyl Ammonium bromide (CTAB), L-Cysteine and Sodium Hydroxide (NaOH). All the glassware used during the experimental work were acid washed. The chemical reagents used were analytical reagent grade

without further purification. Ultra-pure deionized water (Seralpur delta UV/UF setting, 0.055 mS/cm) used in all synthesis steps.

Material synthesis

The photo luminescent, CTAB capped ZnS NPs synthesized in the aqueous micellar solution of the CTAB was steady for quite a long time together. ZnS NPs were readied utilizing basic compound precipitation strategy. In run of the mill try different things with some change, The CTAB micellar solution containing $\text{Na}_2\text{S} \cdot x\text{H}_2\text{O}$ (0.5 M, pH 12.5) was added drop wise to another contains $\text{ZnSO}_4 \cdot 7\text{H}_2\text{O}$ solution (0.5M, pH 2.75, in 0.01M HCl), $\text{S}^{2-}/\text{Zn}^{2+}$ proportion of 2.0 with proceeding vigorous magnetic stirring in laboratory condition. After the Na_2S infusion, white voluminous precipitates appeared during process and pH gradually increases from 3.0 to 8.0. During the reaction, $\text{H}_2\text{S}_{(g)}$ was produced at low concentration which was colorless, highly flammable and gave pungent odor similar to that of rotten eggs odor. Byproduct; H_2SO_4 was utilized informally ZnS NPs whereas NaCl was removed by solubilizing in chilled water, conformed by silver test (AgCl gives white cloudy precipitates). The acquired dispersion was purified by centrifuge at 6000 RPM against demineralised water or NaOH (0.01M) prompting dispersions with a pH of either 8.0 or 13.0 by. The precipitates dried in hot air oven at 120°C [1].

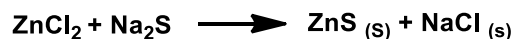
ZnS-L-Cysteine: Core-shell NPs synthesized at laboratory condition. 500 mg CTAB capped ZnS NPs powder dispersed into 100 ml distilled water, alter pH 8.0 of suspension with 0.01 M NaOH solution and ultrasonically scattered for 60 mins. A moderate dropping of 100 ml of 0.5M L-Cysteine aqueous solution (pH 8.0) made into ZnS NPs suspension under magnetic stirring. The nucleation and development of a different L-Cysteine molecule were stifled by the moderate expansion. Following 24 hrs vigorous magnetic stirring, resulting precipitate appears which demonstrate a development of core/shell: ZnS/L-Cysteine NPs and it was purified by centrifuge at 6000 RPM against demineralised water or NaOH (0.01M) prompting dispersions with a pH of either 8.0 or 13.0 by. The precipitates dried in hot air oven at 120°C .

Characterization

The synthesized NPs were characterized using X-ray diffraction (XRD) patterns of the powdered samples using X-ray diffractometer, PTS 3000 by Rich-Seifert instrument with $\text{CuK}\alpha$ radiation ($\lambda = 0.15418 \text{ nm}$) at RT. The size and morphology of the NPs were determined using scanning electron microscope (SEM), Carl Zeiss, Evo-18; 20 kV) images. FTIR spectra of dried powder take with Perkin Elmer spectrum – 65 series FTIR spectrometer. The optical absorption spectra of the NPs in deionized water recorded using UV-2060 plus spectrometer (Over: 200-600 nm). Fluorescence measurements performed on a Hitachi-FP-6500 fluorescence spectrophotometer (Over: 300-500 nm). The thermal gravimetric analysis (TGA) carried out with intercooler Perkin Elmer TGA-6000 thermometer.

Results and discussion

The zinc sulphate (ZnSO_4), sodium sulphide (Na_2S) and CTAB are ionic and their concentration calculated from;



Practically, aqueous (aq.) solution of Na_2S contained both aq. H_2S and HS^- with additional sulphur oxygens [17]. The development of compounds clarified on the premise of Ostwald ripening [18].

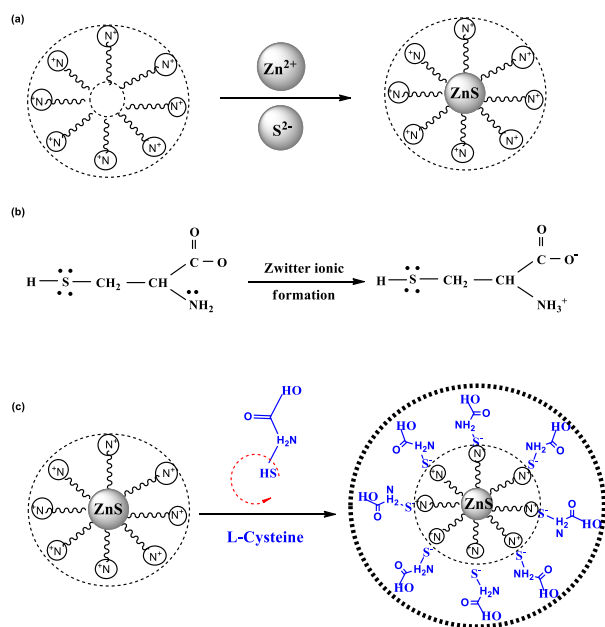


Fig. 1. A model diagram for developing, (a) CTAB capped ZnS NPs, (b) Zwitter ionic formation of L-Cysteine in aq. Solution, (c) ZnS-L-Cysteine: core-shell NPs.

In nucleation, the surface vitality of the particle is high and subsequently passivated by adsorption of anions in the solution (SO_4^{2-} , Cl^- , and S^{2-}). The accumulation of anions thus pulls in cations (Zn^{2+} , Na^+ , and H^+) towards the surface of the particle. Zn^{2+} reacts with S^{2-} and it has consolidated into the crystal lattice of the core (**Fig. 1(a)**). We had developed the new method to effectively coat the L-Cysteine (shell) on CTAB capped ZnS NPs (core). However, adjusting position of functional group of L-Cysteine and CTAB capped ZnS NPs mixture could have accompanied yield by mechanical stirring. The functional group of L-Cysteine could be developed zwitterionic formation during process (**Fig. 1(b)**). L-Cysteine easily coated due to more electronegative S^{2-} atom and stabilized functional groups ($^+\text{NH}_3$ and COO^-) at α - position leads to engaging N^+ of CTAB. It developed local equilibrium theory due to their opposite columbic attraction and distribute the charge to core particle which leads to developing a biocompatible thin coating layer on core particle surface (**Fig. 1(c)**).

The functionalization of ZnS NPs (core) with reactive carboxylic group ($-\text{COOH}$) facilitates its conjugation with various functional proteins, leading to the irreversible

denaturation (or bio-activation) of proteins and potential long-term toxicity [19].

FTIR Study

An IR-spectrum of the precipitate obtained in the range of $4000 - 400 \text{ cm}^{-1}$ for immaculate pure CTAB, CTAB capped ZnS NPs, pure L-Cysteine and ZnS-L-Cysteine: Core-Shell NPs are indicated in **Fig. 2 ((a), (b), (c), (d))**; respectively. It is to be noticed that the symmetric and asymmetric $-\text{CH}_2$ stretching, vibrations of unadulterated CTAB lie at 2917.44 cm^{-1} and 2847.71 cm^{-1} ; remained almost same in the presence of the ZnS NPs within the experimental errors.

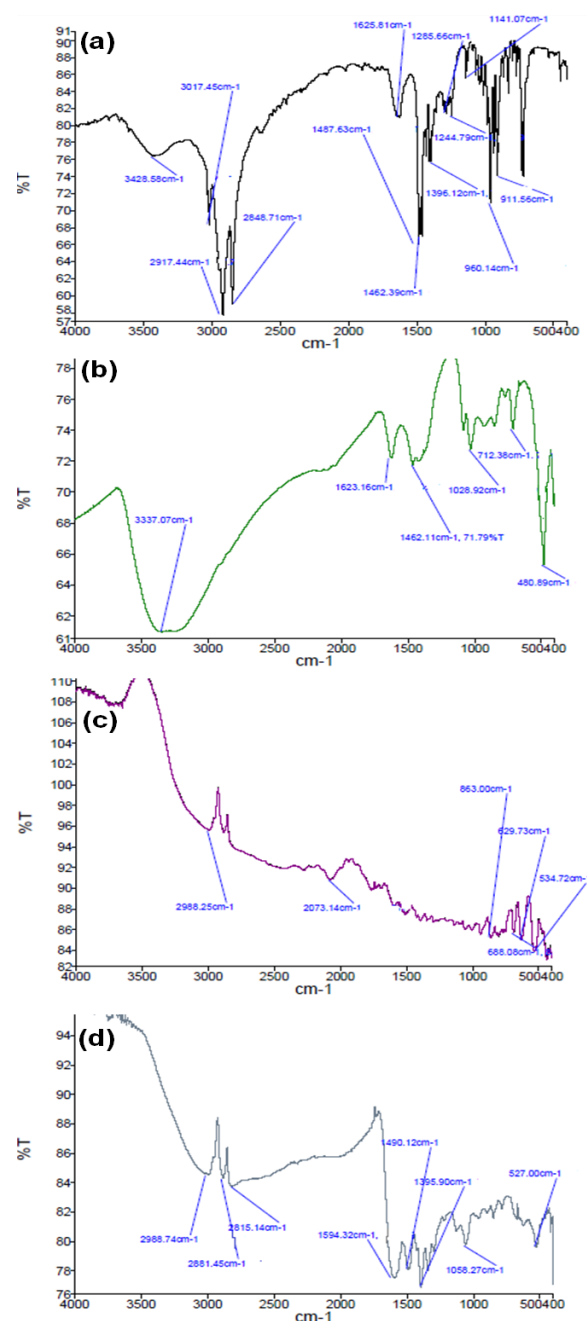


Fig. 2. IR spectra of (a) pure CTAB (b) CTAB capped ZnS NPs (c) pure L-Cysteine and (d) ZnS-L-Cysteine: Core-Shell NPs.

It is to be noticed that the symmetric and asymmetric $-\text{CH}_2$ stretching, Vibrations of unadulterated CTAB lie at

2917.44 cm^{-1} and 2847.71 cm^{-1} ; remained almost same in the presence of the ZnS NPs within the experimental errors. In the pure CTAB spectra $-\text{C}-\text{H}$ scissoring vibrations of $-\text{N}-\text{CH}_3$ moiety peaks shows at 1625.81 cm^{-1} and 1487.63 cm^{-1} , which moved to 1623.16 cm^{-1} and 1462.11 cm^{-1} in the presence of the ZnS NPs. Additionally, the peaks at 1285.66 cm^{-1} and 1244.79 cm^{-1} because of $-\text{C}-\text{N}$ stretching are stifled and essentially moved to 1028.92 cm^{-1} in the presence of ZnS NPs [1]. The district between 1800 cm^{-1} and 300 cm^{-1} obviously show that Cysteine is available as a shell in the NPs structure. At 1587 cm^{-1} and 1531 cm^{-1} we get stretching for a COO^- and NH_3^+ deformation bands which are moved to 1594.32 cm^{-1} and 1490.12 cm^{-1} in the vicinity of the ZnS-L-Cysteine: core-shell NPs, furthermore different bands at lower wave numbers compares well to immaculate Cysteine spectrum.

The NH_3^+ stretch (2073.14 cm^{-1}) band must be expected, and the SH stretch band (2988.25 cm^{-1}) does not exist by any stretch of the imagination. The extensive band range from 2343.13 cm^{-1} to 3178.91 cm^{-1} moved to higher wave numbers. Thus, as shell material Cysteine is a known to form steady complexes with ZnS NPs [20].

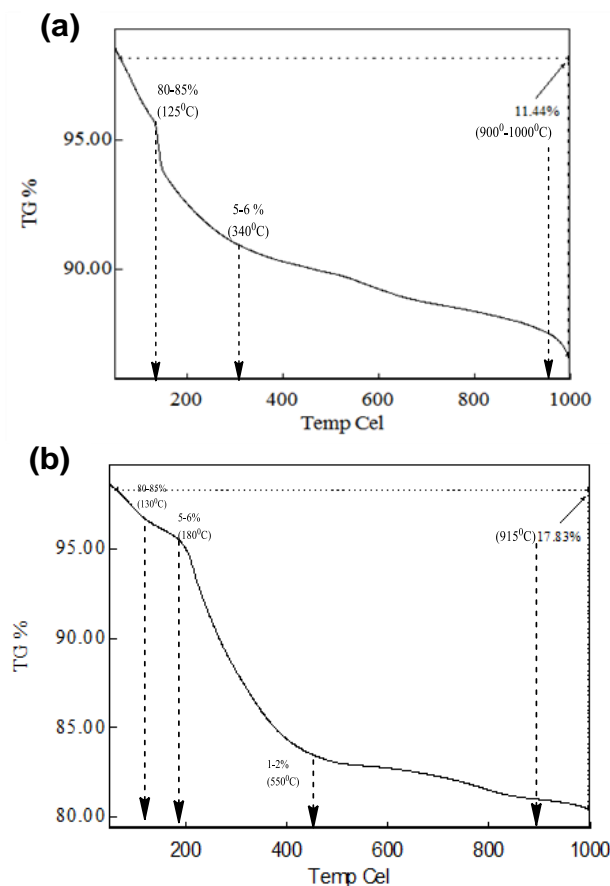


Fig. 3. TGA curve of (a) CTAB capped ZnS NPs (b) ZnS-L-Cysteine: core – shell NPs.

Thermal study

The annealing procedure is compelling for reproducible size control of NPs furthermore it can be utilized to enhance the precious crystal quality and stability which are needed for device purposes. The thermo gravimetric

analysis (TGA) studied for CTAB capped ZnS NPs (**Fig. 3(a)**) and ZnS-L-Cysteine: core-shell NPs (**Fig. 3(b)**) in the temperature ranges from room temperature (RT) to 1,000 °C, which increased by 50 °C /min in an N_2 atmosphere.

In the case of CTAB capped ZnS NPs, molecule abandoned with water, which adsorbed at the particle surface. Subsequently the compound had been isolated from aqueous suspension, due to desorption of water molecules with 80-85 % weight loss was seen at around 125°C and in the second stage around 5-6 % weight loss was seen at around 340 °C because of disintegration of cationic surfactant (CTAB) [21]. Here, toward the end 11.44 % weight loss was seen at around 900-1000 °C due to SO_2 molecules which needs to consider that it starts from the CTAB and the ZnS NPs. Same as in the case of ZnS-L-Cysteine: core-shell NPs, water and CO_2 molecules adsorbed at the particle surface. It already evaporated at temperatures smaller than 100–130 °C. Further, it can start from the carboxylic group of the Cysteine or from CO_2 adsorbed at the particle surface. At temperatures between 180– 300 °C NH_3 evaporates and toward the end between 550 – 915 °C SO_2 .

Here one needs to consider that the SO_2 originates from the Cysteine and the ZnS. Since, the CTAB capped ZnS NPs and ZnS-L-Cysteine: core-shell NPs act as random formation of molecular self-assemblies.

Optical absorption and photoluminescence study

It is a well-established fact that because of quantum confinement of photo generated electron-hole pair, the UV/Vis absorption spectra of semiconductor quantum dots is size dependent [22].

The characteristic absorption peak appears at the maximum wavelength $\lambda_{\text{max}}=265$ nm for CTAB capped ZnS NPs, which indicates 80 nm blue shifted from the bulk ZnS material (345 nm). This blue shift absorption edge is due to the small size of the particle [23]. Similarly, The characteristic absorption peak appears at the maximum wavelength $\lambda_{\text{max}}=290$ nm for ZnS-L-Cysteine: core-shell NPs, which indicates 55 nm blue shift from the bulk ZnS material (345 nm) and 25 nm red shift from the CTAB capped ZnS NPs (265 nm).

Fig. 4 (b) demonstrates the room temperature photoluminescence (PL) range of the redispersed CTAB capped ZnS NPs and ZnS-L-cysteine NPs. It is found that PL property of the uncoated ZnS NPs is verging on identical to that of the samples coated with L-cysteine shell. For all samples, two emission peaks are dominated in the PL spectra. To begin with emission peak centered at 455 nm (blue) and another at 490 nm (these picks should be unquestionably originated from the host ZnS NPs, and one week emission at 425 nm. The fascinating point is that the intensity shows reciprocal trends in spectrum. i.e, the emission which are strong in one become weak in the other and vice-versa. This sort of conduct can be ascribed to change in shape and size of NPs during separation and drying process as the luminescence spectra show size and shape dependent quantum confinement effect.

The CTAB capped ZnS NPs arrangement are surface passivated by abundance sulfide ions and surfactant

monomers and show weak deep-trap (intense shallow-trap) emission at 425 nm, while because of evacuation of passivation after redispersion the defect related emission at 455 nm turned out to be more intense due to deformities in nanocrystals. The peak at 490 nm has been relegated to the vicinity of sulphur vacancies in the lattice [24]. In PL spectra of L-Cysteine coated ZnS NPs (ZnS-L-Cysteine: core-shell NPs), the emission intensity was enormously upgraded at 455 nm turned out to be more intense due to deformities in nanocrystals [25]. Which could be credited to a recombination of electrons at vacant donor level of sulphur with holes trapped at the zinc vacancy acceptor level and it is called recombination mechanism for the framework (Fig. 4(c)). Thus, with core-shell: ZnS-L-Cysteine NPs recombination mechanism the extinguishing of blue emission band is observed [26].

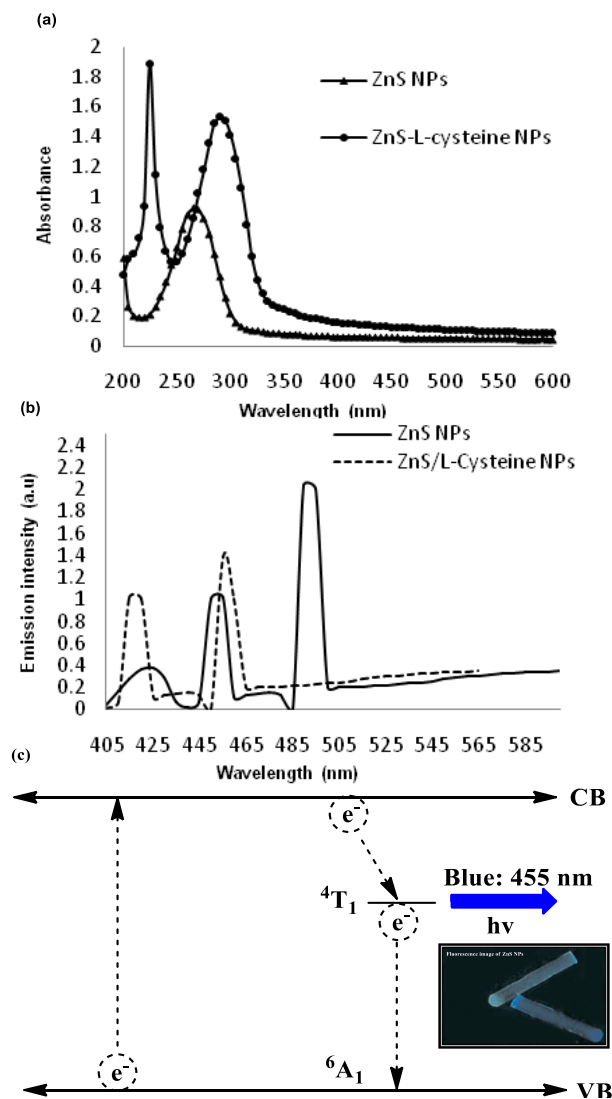


Fig. 4. Spectral characteristic of CTAB capped ZnS NPs and ZnS-L-Cysteine: core-shell NPs, (a) Absorption spectrum, (b) photoluminescence spectra, (c) Recombination mechanism for the framework.

Structure and morphology

Crystallinity, with respect to size and phase of NPs were characterized by XRD analysis. The recorded patterns for

all the samples show in **Fig. 5 ((a), (b))**. Peak positions of the integrated powder demonstrate the development of zinc blende crystal structure with three most preferred orientations (111), (220), and (311). There is no recognizable contamination phase in the spectra, which shows the arrangement of immaculate cubic phase of ZnS only. The broadening of the diffraction peaks divulges the formation of nanosized particles.

In any case, this size compares to the extent of immaculate crystallites, so it can give a thought of the smallest size unit of the crystals. The average nanocrystallites size calculated from FWHM of XRD peaks using Debye-Scherrer's formula; [27]

$$\beta = \frac{\alpha \cdot \lambda}{d \cdot \cos \theta} ; \therefore d = \frac{\alpha \cdot \lambda}{\beta \cdot \cos \theta}$$

where, α is a geometrical factor ($\alpha = 0.94$), λ is the wavelength of X-rays used for analysis ($\lambda = 0.15418$ nm), and β is the full width at half maxima (FWHM) of peaks ($\beta = 0.587$). Here θ corresponding to each plane selected for NPs size calculation. From the calculation, the average diameters for CTAB capped ZnS and ZnS/L-Cysteine: core-shell NPs are 4.40858 ± 0.5 nm and 13.08583 ± 0.5 nm, respectively. However, the observed interplanar spacing (d_{111}) of the ZnS-L-Cysteine: core-shell size essentially expanded than ZnS NPs. It might be because of the presence of a thin shell (L-Cysteine) on the surface of the ZnS NPs.

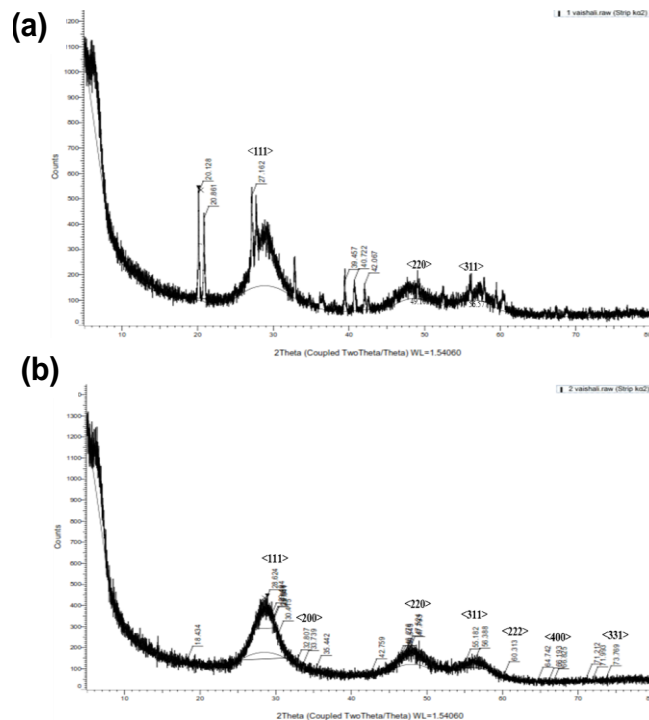


Fig. 5. XRD pattern of (a) CTAB capped ZnS NPs (b) ZnS-L-Cysteine: core-shell NPs.

Morphology of the NPs and particularly the development of the shell are characterized by SEM. **Fig. 6 ((a), (b))** shows the SEM images of CTAB capped ZnS NPs and **Fig. 6 ((c), (d))** shows the SEM images of ZnS-

L-Cysteine: core-shell NPs with same magnifications scale (200 nm). As could be seen, the CTAB capped ZnS and ZnS-L-Cysteine: core-shell NPs sizes assessed to be about 59.76 nm and 78.84 nm range with spherical shape. This outcome discovered to be great concurrence with XRD result. As indicated in **Fig. 6** the synthesized NPs have been extensively aggregated, which may be due to the non-linearity of organic or inorganic surfactant capping on the particles surface.

Fig. 6 (c) demonstrates an intriguing morphology structure of ZnS-L-Cysteine: core-shell NPs. The dark parts in the corners demonstrate the structure like a trunk of a tree. The developments of the NPs appear to be as a few leafs and stem- like structures. Additionally, it could be found in some bit of the image that leafs are specifically expanded from the root. Accordingly, the collecting of very small spherical particles appears as root structure with micrometer leafs.

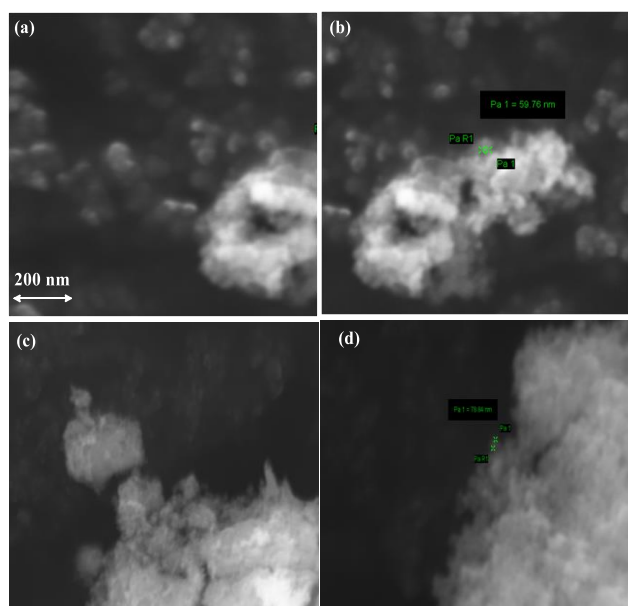


Fig. 6. SEM images at 200 nm magnification scale of (a, b) CTAB capped ZnS NPs and (c, d) ZnS-L-Cysteine: core-shell NPs.

These structures may be due to the gathering of ZnS NPs by amino acid: L-Cysteine. Amazingly, the ZnS NPs passivated with CTAB is very small and the particles have exceptionally narrow size appropriation. In addition, the particles intensity (number of the particles formed in square centimeter) implies the change of growth rate without aggregation.

In-situ opto-electronic properties

Opto-electronic properties analysed by dynamic light scatter (DLS) at pH 8.0. The synthesized CTAB capped ZnS NPs have negative polarity on the surface with -23.96 mV zeta-potential and -0.03897 fC surface charges. Due to quantum confinement effect NPs act as semiconducting material with 32 μ S/cm conductivity and higher refractive index 2.333. Same as, synthesized ZnS-L-Cysteine: core-shell NPs have also negative polarity on the surface with -24.54mV zeta-potential and -0.04002 fC surface charges. Due to quantum confinement effect NPs

act as semiconducting material with 92 μ S/cm conductivity and higher refractive index 1.237.

Conclusion

Out of different II – VI direct band gap semiconductor, ZnS and in addition a CTAB capped ZnS NP has high refractive index and multi photon absorption attributes as mulled over in this paper. ZnS NPs emit blue emission light when excited to UV radiation and these noticeable PL emission spectra distinguished effectively with exposed eye. In this manner, water-soluble ZnS NPs synthesized by the introduced strategy may be contender for potential application in optoelectronics devices. On the other hand, for biophotonics devices, the synthesized NPs functionalized with suitable materials for making them biodynamic and to hold their size, shape and physical properties particularly optical and photoluminescence after they are labeled with biomolecules. In this way, combined CTAB capped ZnS NPs functionalized with L-Cysteine (Amino acid) resultant ZnS-L-Cysteine: core-shell NPs making surface bioactive with effortless water-soluble which simple to use in creation of biophotonics devices.

Acknowledgements

Authors are thankful to Central University of Gujarat, Gandhinagar, for infrastructural support and thankful to Gujarat Forensic Science University, Gujarat for fluorescence spectroscopy and Department of forensic science (DFS), Gujarat for SEM analysis.


Supporting information

Supporting informations are available from VBRI Press.

References

- Shukla, V.; Singh, M.; *AIP Conference Proceedings*, **2016**, 1724, 020126.
- Chaudhuri, R.G. and Paria, S.; *Chem. Rev.*, **2012**, 112, 2373.
- Srdić, V.V.*; Mojić, B.; Nikolić, M.; Ognjanović, S.; *Processing and Application of Ceramics*, **2013**, 7, 45.
- Colvin, V.L.; Schlamp, M.C.; Alivisatos, A.P.; *Letters to Nature*, **1994**, 370, 354.
- Mitchell, G.P.; Mirkin, C.A.; Letsinger, R.L.; *J Am Chem Soc*, **1999**, 121, 8122.
- Gao, M.; Rogach, A.L.; Kornowski, A.; Kirstein, S.; Eychmuller, A.; Mohwald, H.; Weller, H.; *J Phys Chem B*, **1998**, 102, 8360.
- Nomoev, A. V.; Bardakhanov, S. P.; Schreiber, M.; Bazarova, D. G.; Romanov, N. A.; Baldanov, B. B.; Radnaev, B. R. and Syzrantsev, V. V.; *Beilstein J. of Nanotechnology*, **2015**, 6, 874.
- Miki, I.; Hiroki, K.; Iwao, H.; Yoshikazu, H.; *Material Express*, **2013**, 3, 355.
- Miki, I.; Hiroki, K.; Iwao, H.; Yoshikazu, H.; *Material Express*, **2014**, 4, 135.
- Embsen, J. V.; Jasieniak, J.; Gómez, D. E.; Mulvaney, P.; Giersig, M.; *Australian J. of Chemistry*, **2007**, 60, 457.
- Mehta, S. K.; Kumar, S.; Chaudhary, S.; Bhasin, K. K.; and Gradzielski, M.; *Nanoscale Res Lett.*, **2009**, 4, 17.
- Chen R. and Lockwood, D. J.; *J. Electrochem. Soc.*, **2002**, 149, S69.
- Warad, H. C.; Ghosh, S. C.; Hemtanon, B.; Thanachayanont, C.; and Dutta, J.; *Science and Technology of Advanced Materials*, **2005**, 6, 296.
- Sana, P.; Hashmi, L.; and Malik, M. M.; *International Scholarly Research Network, ISRN Optics*, **2012**, 2012.
- Ruitao, L.v.; Cao, C.; Guo, Y.; and Zhu, H.; *J. Mater. Sci.*, **2004**, 39, 1575.
- Wang, X.; Xu, H.; Liu, H.; Schelly, Z. A.; and Wu, S.; *Nanotechnology*, **2007**, 18, 15.

17. Zhang, X. V.; Ellery, S. P.; Friend, C. M.; Holland, H. D.; Michel, F. M.; Schoonen, M. A. A.; Martin, S. T.; *J. Photochem. Photobiol.Chem.*, **2004**, 168, 153.
18. Yao, J. H.; Elder, K. R.; Guo, H.; Grant, M.; *Phys. Rev. B*, **1993**, 47, 14110.
19. Mu, Li.; Gao, Yue.; Xiangang, Hu.; *Journal of biomaterials*, **2015**, 52, 301.
20. Vieira, A.P.; Berndt, G.; de Souza Junior; I.G. et al.; *Amino Acids*, **2011**, 40, 205.
21. Mishra, D.; Prabhakar, P.; Lahiri, S.; Amriphale, S. S.; and Chandra, N.; *Indian journal of chemistry*, **2013**, 52-A, 1591.
22. Huang, N.M.; Kan, C.S.; Khiew, P.S. et al. ; *Journal of Materials Science*, **2004**, 39, 2411.
23. Wang, Y.; Suna, A.; Mahler, W.; Kasowaki, R.; *J. Chem. Phys.*, **1987**, 87, 7315.
24. Maity, R.; Chattopadhyay, K. K.; *Nanotechnology*, **2004**, 15, 812.
25. Murugadoss, G.; Rajamannan, B.; Ramasamy, V.; *Journal of Luminescence*, **2010**, 130-11, 2032.
26. Taheri Otaqsara, S.M.; *Eur. Phys. J. Appl. Phys.*, **2012**, 59, 10404.
27. Murugadoss, G.; *Appl Nanosci*, **2013**, 4853.



Advanced Materials Letters

Volume 8, February 2017

As official journal of International Association of Advanced Materials
www.iaaamonline.org

Available online at
www.vbripress.com/aml

A Monthly Journal

Publish your article in this journal

Advanced Materials Letters is an official international journal of International Association of Advanced Materials (IAAM, www.iaaamonline.org) published monthly by VBRI Press AB from Sweden. The journal is intended to provide high-quality peer-review articles in the fascinating field of materials science and technology particularly in the area of structure, synthesis and processing, characterisation, advanced-state properties and applications of materials. All published articles are indexed in various databases and are available download for free. The manuscript management system is completely electronic and has fast and fair peer-review process. The journal includes review article, research article, notes, letter to editor and short communications.

VBRI Press
Commitment to Excellence

www.vbripress.com/aml

Copyright © 2016 VBRI Press AB, Sweden

Supporting information

Table 1. Applicable surfactants for the NPs synthesis.

Surfactants	Comment on its nature
Alginic acid	Low concentration, NPs cannot be isolated
CTAB	High concentrations, dispersions stable for 3-4 weeks NPs can be isolated and good PL- properties
Hexametaphosphate	Stable for 2-3 days
Hydroxypropyl cellulose	Stable dispersion, but poor PL- properties
Mercaptopropionic acid	Corrodes plastic parts
Polymethacrylic acid	Particles precipitate embedded in polymer matrix, cannot be dispersed
Polyvinyl alcohol	Stable for 2-3 days
Polyvinyl pyrrolidone	Stable dispersions, low concentrations, NPs cannot be isolated
Thioglycerole	Basic pH needed for stabilization leads to $\text{Zn}(\text{OH})_2$ precipitation before addition of Na_2S
TWEEN 80	Highly stable, but poor PL- properties